Article

Naked (CMe)M Cations (M = Sc, Ti, and V) and Their Fluoroarene Complexes

Marco W. Bouwkamp, Peter H. M. Budzelaar, Jeroen Gercama, Isabel Del Hierro Morales, Jeanette de Wolf, Auke Meetsma, Sergei I. Troyanov, Jan H. Teuben, and Bart Hessen

J. Am. Chem. Soc., **2005**, 127 (41), 14310-14319• DOI: 10.1021/ja054544i • Publication Date (Web): 23 September 2005

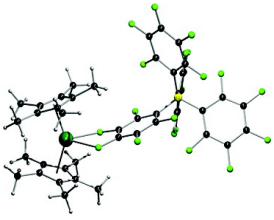

$[Cp^*_2Sc(\kappa F^2\text{-}C_6F_5)B(C_6F_5)_3]$
κF^2 w/ counterion

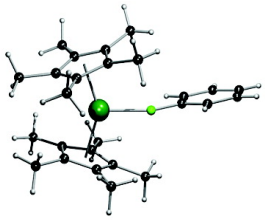

$[Cp^*_2Ti(\kappa F\text{-}FC_6H_5)][B(C_6F_5)_4]$
κF w/ fluorobenzene

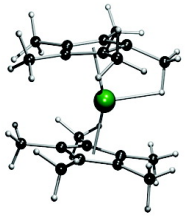

$[Cp^*_2V][B(C_6F_5)_4]$
agostic w/ Cp* ligand

More About This Article

Additional resources and features associated with this article are available within the HTML version:

- Supporting Information
- Links to the 9 articles that cite this article, as of the time of this article download
- Access to high resolution figures
- Links to articles and content related to this article
- Copyright permission to reproduce figures and/or text from this article

View the Full Text HTML

J|A|C|S
ARTICLES
Published on Web 09/23/2005

Naked $(C_5Me_5)_2M$ Cations (M = Sc, Ti, and V) and Their Fluoroarene Complexes

Marco W. Bouwkamp,[†] Peter H. M. Budzelaar,[‡,||] Jeroen Gercama,[†] Isabel Del Hierro Morales,[†] Jeanette de Wolf,[†] Auke Meetsma,[†] Sergei I. Troyanov,[§] Jan H. Teuben,[†] and Bart Hessen*[,†]

Contribution from the Center for Catalytic Olefin Polymerization, Stratingh Institute for Chemistry and Chemical Engineering, University of Groningen, Nijenborgh 4, 9747 AG, Groningen, The Netherlands, Molecular Materials, Radboud University Nijmegen, P.O. Box 9010, 6500 GL, Nijmegen, The Netherlands, and Department of Chemistry, Moscow State University, Vorobjovy Gory, 119899 Moscow, Russia

Received July 20, 2005; E-mail: B.Hessen@chem.rug.nl

Abstract: The ionic metallocene complexes $[Cp^*_2M][BPh_4]$ ($Cp^* = C_5Me_5$) of the trivalent 3d metals Sc, Ti, and V were synthesized and structurally characterized. For M = Sc, the anion interacts weakly with the metal center through one of the phenyl groups, but for M = Ti and V, the cations are naked. They each contain one strongly distorted Cp* ligand, with one (V) or two (Ti) agostic C−H···M interactions involving the Cp*Me groups. For Sc and Ti, these Lewis acidic species react with fluorobenzene and 1,2-difluorobenzene to yield $[Cp^*_2M(\kappa F\text{-}FC_6H_5)_n][BPh_4]$ (M = Sc, $n = 2$; M = Ti, $n = 1$) and $[Cp^*_2M(\kappa^2 F\text{-}1,2\text{-}F_2C_6H_4)][BPh_4]$, the first examples of κF-fluorobenzene and $\kappa^2 F$-1,2-difluorobenzene adducts of transition metals. With the perfluorinated anion $[B(C_6F_5)_4]^-$, both Sc and Ti form $[Cp^*_2M(\kappa^2 F\text{-}C_6F_5)B(C_6F_5)_3]$ contact ion pairs. The nature of the metal−fluoroarene interaction was studied by density functional theory (DFT) calculations and by comparison with the corresponding tetrahydrofuran (THF) adducts and was found to be predominantly electrostatic for all metals studied.

Introduction

As a result of the relative inertness of the C−F bond[1] and the high electronegativity of fluorine,[2] and the fact that the radius of fluorine is not much larger than that of hydrogen,[3] fluorinated groups are widely applied in transition-metal-based homogeneous catalysis. They can be used as substituents on the ancillary ligand set, for example, to modify the electronic properties of the metal center[4] or the solubility of the catalyst.[5] Another important application of fluorinated moieties is found in weakly nucleophilic anions used in conjunction with (often highly electron deficient) cationic transition-metal catalysts. This is particularly important in catalytic olefin polymerization,[6] where the counterion can strongly influence catalyst productivity and selectivity.[7,8]

Despite their importance to catalysis, interactions of fluorinated groups with highly electrophilic transition-metal centers[9] have not been studied in a systematic fashion, and structurally characterized examples of transition-metal complexes with direct C−F···M interactions involve either intramolecular interactions, where the fluorinated group forms an integral part of the ligand system,[10] or the closest contacts between a cationic transition-metal complex and its fluorinated organoborate counterion.[11]

In this paper, we describe a combined experimental and

[†] University of Groningen.
[‡] Radboud University Nijmegen.
[||] Current address: Department of Chemistry, University of Manitoba, Winnipeg, Manitoba R3T 2N2, Canada.
[§] Moscow State University.

(1) Eggar, K. W.; Cocks, A. T. *Helv. Chim. Acta* **1973**, *56*, 1516.
(2) The electronegativity of fluorine on the Pauling scale: 3.98. *The Nature of the Chemical Bond and the Structure of Molecules and Crystals: an Introduction to Modern Structural Chemistry*; Pauling, L., Ed.; Cornell University Press: Ithaca, NY, 1960.
(3) . *Handbook of Chemistry and Physics*, 80th edition; Lide, D. R., Ed.; CRC Press: Boca Raton, FL, 1999−2000.
(4) (a) Tsukahara, T.; Swenson, D. C.; Jordan, R. F. *Organometallics* **1997**, *16*, 3303. (b) Brussee, E. A. C.; Meetsma, A.; Hessen, B.; Teuben, J. H. *Chem. Commun.* **2000**, 497. (c) Saito, J.; Mitani, M.; Onda, M.; Mohri, J.-I.; Ishii, S.-I.; Yoshida, Y.; Nakano, T.; Tanaka, H.; Matsugi, T.; Kojoh, S.-I.; Kashiwa, N.; Fujita, T. *Macromol. Rapid Commun.* **2001**, *22*, 1072. (d) Mitani, M.; Mohri, J.-I.; Yoshida, Y.; Saito, J.; Ishii, S.; Tsuru, K.; Matsui, S.; Furuyama, R.; Nakano, T.; Tanaka, H.; Kojoh, S.-I.; Matsugi, T.; Kashiwa, N.; Fujita, T. *J. Am. Chem. Soc.* **2002**, *124*, 3327. (e) Thornberry, M. P.; Reynolds, N. T.; Deck, P. A.; Fronczek, F. R.; Rheingold, A. L.; Liable-Sands, L. M. *Organometallics* **2004**, *23*, 1333.
(5) (a) Horváth, I. T.; Rábai, J. *Science* **1994**, *266*, 72. (b) De Wolf, E.; Van Koten, G.; Deelman, G.-J. *Chem. Soc. Rev.* **1999**, *28*, 37. (c) Arthel-Rosa, L. P.; Gladysz, J. A. *Coord. Chem. Rev.* **1999**, *190*−*192*, 587.
(6) For reviews on catalytic olefin polymerization with transition-metal complexes see: (a) Möhring, P. C.; Coville, N. J. *J. Organomet. Chem.* **1994**, *479*, 1. (b) Brintzinger, H. H.; Fischer, D.; Mülhaupt, R.; Rieger, B.; Waymouth, R. M. *Angew. Chem., Int. Ed.* **1995**, *34*, 1143. (c) Britovsek, G. J. P.; Gibson, V. C.; Wass, D. F. *Angew. Chem., Int. Ed.* **1999**, *38*, 428. (d) Coates, G. W. *Chem. Rev.* **2000**, *100*, 1223.
(7) (a) Chen, E. Y.-X.; Marks, T. J. *Chem. Rev.* **2000**, *100*, 1391. (b) Piers, W. E.; Irvine, G. J.; Williams, V. C. *Eur. J. Inorg. Chem.* **2000**, 2131. (c) Pédeutour, J.-N.; Radhakrishnan, K.; Cramail, G.; Deffieux, A. *Macromol. Rapid Commun.* **2001**, *22*, 1095.
(8) (a) Chen, Y.-X.; Metz, M. V.; Li, L.; Stern, C. L.; Marks, T. J. *J. Am. Chem. Soc.* **1998**, *120*, 6287. (b) Metz, M. V.; Schwartz, D. J.; Stern, C. L.; Marks, T. J.; Nickias, P. N. *Organometallics* **2002**, *21*, 4159.
(9) (a) Kulawiec, R. J.; Crabtree, R. H. *Coord. Chem. Rev.* **1990**, *99*, 89. (b) Plenio, H. *Chem. Rev.* **1997**, *97*, 3363.
(10) (a) Siedle, A. R.; Newmark, R. A.; Lamanna, W. M.; Huffman, J. C. *Organometallics* **1993**, *12*, 1491. (b) Burlakov, V. V.; Pellny, P.-M.; Arndt, P.; Baumann, W.; Spannenberg, A.; Shur, V. B.; Rosenthal, U. *Chem. Commun.* **2000**, 241.

10.1021/ja054544i CCC: $30.25

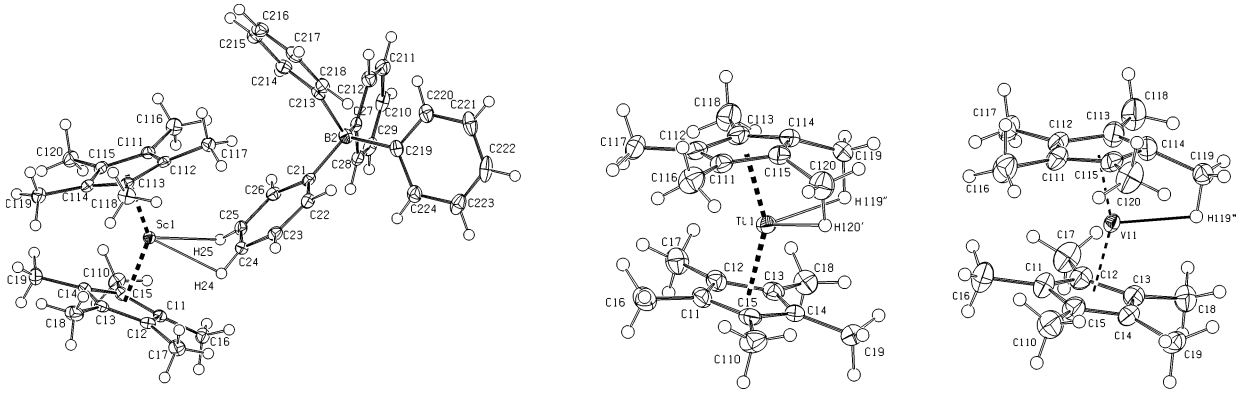

Figure 1. ORTEP representation of **1a,b** and the major fraction of **1c** showing 50% probability ellipsoids. The anions of **1b,c** are omitted for clarity.

Scheme 1

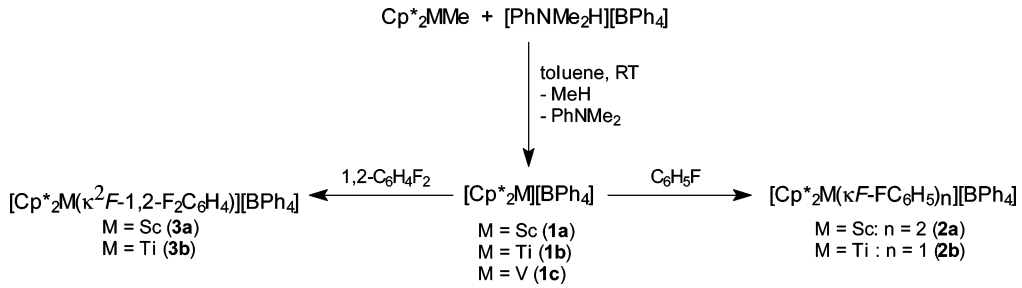

density functional theory (DFT) theoretical study of the electron-deficient decamethylmetallocene cations of the trivalent 3d metal ions of scandium (d^0), titanium (d^1), and vanadium (d^2), as well as their interaction with fluorobenzene, 1,2-difluorobenzene, and the $[B(C_6F_5)_4]$ anion. For comparison, the interaction of the cations with the "classic" Lewis base tetrahydrofuran (THF) was studied. Here, we report the unusual structural behavior of the "naked" decamethylmetallocene cations, as well as the first examples of isolated κF-fluorobenzene and $\kappa^2 F$-1,2-difluorobenzene adducts of transition metals. Experimental and theoretical results suggest that the metal−fluoroarene interaction in these complexes is predominantly electrostatic. Some aspects of the titanium system were communicated previously.[12]

Results

Synthesis of Base-Free Decamethylmetallocene Cations. The base-free decamethylmetallocene cations can be prepared as their tetraphenylborate salts, $[Cp^*_2M][BPh_4]$ (**1a**−**c**), by reaction of Cp^*_2ScMe,[13] Cp^*_2TiMe,[14] or Cp^*_2VMe[15] with the Brønsted acid $[PhNMe_2H][BPh_4]$[16] in toluene (Scheme 1). This reaction results in a yellow precipitate in the case of scandium and a brown precipitate in the case of titanium or vanadium. Recrystallization of the base-free metallocene cations is impeded by their poor solubility in aliphatic or aromatic solvents and by their reactivity toward most other solvents. Nevertheless, when these reactions are performed without stirring, the generation of the scandocene and titanocene cations **1a,b** in toluene results in precipitation of yellow (**1a**) or red (**1b**) crystals, suitable for X-ray diffraction, directly from the reaction mixture. The base-free decamethylvanadocene cation **1c** could be successfully recrystallized from 1,2-difluorobenzene/cyclohexane. The compounds were characterized by X-ray diffraction, by elemental analysis, and by their reaction with THF, which cleanly afforded the corresponding THF adducts **5a**−**c** (vide infra).

Table 1. Selected Bond Distances (Å) and Angles (deg) for **1a**

Sc(1)−Cp*(1)[a]	2.1516(10)	C(21)−C(22)	1.420(3)
Sc(1)−Cp*(2)[b]	2.1587(9)	C(21)−C(26)	1.406(3)
Sc(1)−H(24)	2.35(2)	C(22)−C(23)	1.379(3)
Sc(1)−H(25)	2.67(2)	C(23)−C(24)	1.400(3)
Sc(1)−C(24)	2.679(2)	C(24)−C(25)	1.397(3)
Sc(1)−C(25)	2.864(2)	C(25)−C(26)	1.400(3)
Cp*(1)−Sc(1)−Cp*(2)	140.94(4)	C(21)−B(2)−C(27)	115.44(17)
Cp*(1)−Sc(1)−H(24)	128.5(6)	C(21)−B(2)−C(213)	100.45(16)
Cp*(1)−Sc(1)−H(25)	117.3(5)	(C21)−B(2)−C(219)	109.91(16)
Cp*(2)−Sc(1)−H(24)	87.2(6)	C(27)−B(2)−C(213)	112.36(16)
Cp*(2)−Sc(1)−H(25)	95.2(4)	C(27)−B(2)−C(219)	106.00(16)
Sc(1)−H(24)−C(24)	99.6(16)	C(213)−B(2)−C(219)	112.86(16)
Sc(1)−H(25)−C(25)	92.2(15)	∠{BC−Ph}[c]	9.02(12)
		∠(ScH_2,PhB)[d]	58.0(9)

[a] Cp*(1) is the centroid of the C(11)−C(15) ring. [b] Cp*(2) is the centroid of the C(111)−C(115) ring. [c] ∠{B(2)−C(213),C(213) > C(218)} is defined as the angle between the B(2)−C(213) bond and the phenyl ring including C(213)−C(218). [d] ∠(ScH_2,PhB) is defined as the angle between the Sc(1)−H(24)−H(25) and PhB planes.

Structures of the Base-Free Decamethylmetallocene Cations. ORTEP representations of the metallocene cations **1a**−**c** are depicted in Figure 1 (see Table 1 and Table 2 for a selection of bond lengths and angles). The $[Cp^*_2Sc]$ cation adopts a normal bent-metallocene geometry (Cp*(1)−Sc(1)−Cp*(2) = 140.94(4)°). One phenyl group of the $[BPh_4]$ anion in **1a** shows a close contact with the metal center (Sc(1)−H(24) = 2.35(2), Sc(1)−H(25) = 2.67(2) Å; Sc(1)−C(24) = 2.679(2), Sc(1)−

(11) (a) Yang, X.; Stern, C. L.; Marks, T. J. *Organometallics* **1991**, *10*, 840. (b) Horton, A. D.; Orpen, A. G. *Organometallics* **1991**, *10*, 3910. (c) Yang, X.; Stern, C. L.; Marks, T. J. *J. Am. Chem. Soc.* **1994**, *116*, 10015.
(12) Bouwkamp, M. W.; De Wolf, J.; Del Hierro Morales, I.; Gercama, J.; Meetsma, A.; Troyanov, S. I.; Hessen, B.; Teuben, J. H. *J. Am. Chem. Soc.* **2002**, *124*, 12956.
(13) Thompson, M. E.; Baxter, S. M.; Bulls, A. R.; Burger, B. J.; Noltemeyer, M.; Santarsiero, B. D.; Schaefer, W. P.; Bercaw, J. E. *J. Am. Chem. Soc.* **1987**, *109*, 203.
(14) Luinstra, G. A.; Ten Cate, L. C.; Heeres, H. J.; Pattiasina, J. W.; Meetsma, A.; Teuben, J. H. *Organometallics* **1991**, *10*, 3227.
(15) Curtis, C. J.; Smart, C.; Robbins, J. L. *Organometallics* **1985**, *4*, 1283.
(16) Eshuis, J. J. W.; Tan, Y. Y.; Meetsma, A.; Teuben, J. H.; Renkema, J.; Evens, G. G. *Organometallics* **1992**, *11*, 362.

Table 2. Selected Bond Distances (Å) and Angles (deg) for **1b,c**

	1b	1c
M(1)−Cp*(1)[a]	1.9596(14)	1.9228(14)
M(1)−Cp*(2)[b]	1.9796(14)	1.8845(14)
M(1)−C(111)	2.352(3)	2.219(3)
M(1)−C(112)	2.471(3)	2.260(3)
M(1)−C(113)	2.353(3)	2.303(3)
M(1)−C(114)	2.159(3)	2.303(3)
M(1)−C(115)	2.167(3)	2.258(3)
M(1)−H(119″)	2.16(3)	2.06(3)
M(1)−H(120′)	2.20(3)	
C(114)−C(119)	1.502(5)	1.501(4)
C(115)−C(120)	1.486(5)	
C(114)−(C115)	1.434(4)	
Cp*(1)−M(1)−Cp*(2)	151.00(6)	155.00(7)
∠{Cp*(1),C(114)−C(119)}[c]	24.9(3)	26.1(3)
∠{Cp*(1),C(115)−C(120)}[d]	23.6(3)	

[a] Cp*(1) is the centroid of the C(111)−C(115) ring. [b] Cp*(2) is the centroid of the C(11)−C(15) ring. [c] ∠{Cp*(1),C(114)−C(119)} is defined as the angle between the Cp*(1) plane and the C(114)−C(119) bond. [d] ∠{Cp*(1),C(115)−C(120)} is defined as the angle between the Cp*(2) plane and the C(115)−C(120) bond.

C(25) = 2.864(2) Å). This interaction does not lead to a significant distortion of the phenyl group, but some deviation from the ideal tetrahedral surrounding of the boron atom is evident from the C(21)−B(2)−C(213) angle of 100.45(16)°.

A comparable interaction with phenyl groups of the tetraphenylborate anion is observed in the salts [Cp*$_2$M(η^2-Ph)$_2$BPh$_2$] (M = Sm and U),[17] where the larger ionic radius of the Sm^{3+} and U^{3+} cations allows for the binding of two phenyl groups.[18] For [{C_2H_4(Ind)$_2$}ZrMe(η^2-Ph)BPh_3] (Ind = indenyl), the coordination of a single phenyl group of the anion was proposed on the basis of solution NMR data.[19]

The molecular structures of **1b** and **1c** show no interactions between the anion and the metal center. Instead, the naked cations both contain one highly distorted Cp* ligand. The titanium complex **1b** (Figure 1, Table 2) has one normal η^5-bound Cp* ligand and one having two agostic C−H···Ti interactions of adjacent methyl groups with the metal center (Ti(1)−H(119″) = 2.16(3) Å; Ti(1)−H(120′) = 2.20(3) Å). The relevant C_{Cp}−C_{Me} distances represent single bonds and clearly rule out formation of a metalated Cp* ligand.[20] The two agostic methyl groups are directed toward the metal center (deviation of the C−Me bonds from the Cp* plane: 24.9(3) and 23.6(3)°), and the Cp* ligand with the agostic interaction is slipped back so that Ti(1)−C(114) and Ti(1)−C(115) are the shortest Ti−C bond distances in the molecule. Nevertheless, the intraligand C−C bond distances are normal for a Cp* ligand.

The vanadium complex **1c** crystallized in the $P\bar{1}$ space group with two molecules of [Cp*$_2$V][BPh_4] in the asymmetric unit. Refinement was complicated by a disorder problem (see Supporting Information). An ORTEP representation of the major fraction of one of the crystallographically independent cations of **1c** is depicted in Figure 1; pertinent bond distances and angles are listed in Table 2. Compound **1c** has one normal η^5-bound Cp* ligand and one having a single agostic C−H···V interaction of a Cp* methyl group with the metal center. This methyl group is directed toward the metal center in a manner similar to that observed in the base-free titanocene cation, **1b**, with an angle of 26.1(3)° between the Cp* plane and the C(11)−(C16) bond. The Cp* ligand with the agostic interaction is again slipped back, though the intraligand C−C bond distances are normal for a Cp* ligand.

Reaction of Base-Free Metallocene Cations with Fluoroarenes. Dissolution of the decamethylmetallocene cations of scandium and titanium (**1a,b**) in fluorobenzene results in clear solutions from which, respectively, yellow or green crystals precipitated upon layering with aliphatic solvents. The compounds were characterized by single-crystal X-ray diffraction as the bis- and mono-κF-fluorobenzene adducts [Cp*$_2$Sc(κF-FC_6H_5)$_2$][BPh_4] (**2a**) and [Cp*$_2$Ti(κF-FC_6H_5)][BPh_4] (**2b**), respectively (Scheme 1). Under similar conditions, reaction of the decamethylscandocene and -titanocene cations with 1,2-difluorobenzene results in the $\kappa^2 F$-1,2-difluorobenzene adducts [Cp*$_2$Sc($\kappa^2 F$-1,2-$F_2C_6H_4$)][BPh_4] (**3a**) and [Cp*$_2$Ti($\kappa^2 F$-1,2-$F_2C_6H_4$)][BPh_4] (**3b**). The coordinated molecules of fluorobenzene and 1,2-difluorobenzene are readily displaced by THF; the ^{1}H and ^{19}F NMR spectra of complexes **2a,b** and **3a,b** in THF-d_8 correspond to a mixture of the THF adducts **5a,b** (vide infra) and free fluorobenzene or 1,2-difluorobenzene, respectively. The [Cp*$_2$V] cation does not react with fluorobenzene or 1,2-difluorobenzene. Precipitation of the decamethylvanadocene cation from fluorobenzene or recrystallization from 1,2-difluorobenzene results in recovery of base-free **1c**.

Structure of the Fluorobenzene and 1,2-Difluorobenzene Adducts. ORTEP representations of the κF-fluorobenzene adducts **2a,b** are depicted in Figure 2 (see Table 3 for pertinent bond distances and angles). The M−F bond distances (M = Sc, 2.2725(17) and 2.2884(16) Å; M = Ti, 2.151(2) Å) are longer than those in the neutral, trivalent metallocene fluoride complexes (M = Sc, 2.05(2) Å;[21] M = Ti, 1.845(4) Å[22]) but shorter than those in, e.g., the contact ion pair [(nacnac)ScMe]-[(μ-Me)B(C_6F_5-κF^1)(C_6F_5)$_2$] ((nacnac = (2,6-$(CHMe_2)_2C_6H_3$)-NC(*t*-Bu)CHC(*t*-Bu)N(2,6-$(CHMe_2)_2C_6H_3$)), Sc−F = 2.390(4) Å)[23] or the zwitterionic titanium(III) complex Cp*[η^5-C_5Me_4-CH_2B(κF-C_6F_5)$_2$(C_6F_5)Ti] (Ti−F = 2.406 Å). The C−F bonds in the coordinated fluorobenzene (**2a** = 1.408(3) and 1.414(3) Å; **2b** = 1.402(3) Å) are elongated relative to free fluorobenzene (C−F = 1.3640(16) Å).[24] The M−F−C angles in both **2a** (172.21(16) and 165.27(15)°) and **2b** (168.8(2)°) are close to linear.

The X-ray structures of the 1,2-difluorobenzene adducts **3a,b** are represented in Figure 3 (Table 4 contains pertinent bond distances and angles). The overall geometries of the two cations are very similar even though the compounds are not isomorphous. In the scandium compound, both M−F bond distances are equal (2.330(2) Å) and are longer than those in the κF-fluorobenzene adducts **2a** (2.2725(17) and 2.2884(16) Å). In the Ti compound, the two M−F distances differ significantly

(17) (a) Evans, W. J.; Seibel, C. A.; Ziller, J. W. *J. Am. Chem. Soc.* **1998**, *120*, 6745. (b) Calderazzo, F.; Ferri, I.; Pampaloni, G. *Organometallics* **1999**, *18*, 2452. (c) Evans, W. J.; Nyce, G. W.; Forrestal, K. J.; Ziller, J. W. *Organometallics* **2002**, *21*, 1050.
(18) Shannon, R. D. *Acta Crystallogr.* **1976**, *A32*, 751.
(19) Horton, A. D.; Frijns, J. H. G. *Angew. Chem., Int. Ed.* **1991**, *30*, 1152.
(20) Kupfer, V.; Thewalt, U.; Tišlerová, I.; Štepnička, P.; Gyepes, R.; Kubišta, J.; Horáček, M.; Mach, K. *J. Organomet. Chem.* **2001**, *620*, 39.
(21) Bottomley, F.; Paez, D. E.; White, P. S. *J. Organomet. Chem.* **1985**, *291*, 35.
(22) Lukens, W. W., Jr.; Smith, M. R., III; Anderson, R. A. *J. Am. Chem. Soc.* **1996**, *118*, 1719.
(23) Hayes, P. G.; Piers, W. E.; McDonald, R. *J. Am. Chem. Soc.* **2002**, *124*, 2132.
(24) It should be noted that the C−F bond length observed in the structure of fluorobenzene itself is elongated as well because of C−F···H interactions in the solid state. Thalladi, V. L.; Weiss, H.-C.; Bläser, D.; Boese, R.; Nangia, A.; Desiraju, G. R. *J. Am. Chem. Soc.* **1998**, *120*, 8702.

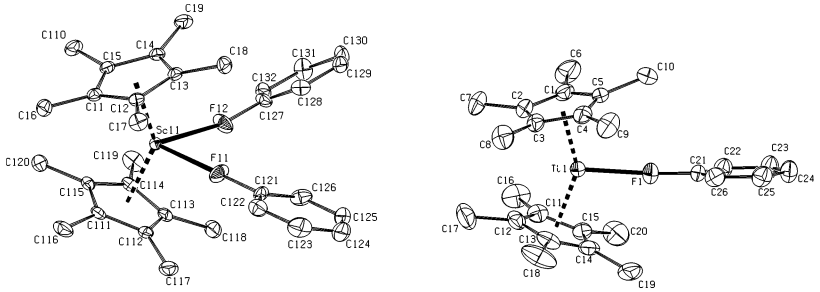

Figure 2. ORTEP representation of the cations of **2a,b** showing 50% probability ellipsoids. The anions and the hydrogen atoms (and the cocrystallized fluorobenzene solvent molecule in **2b**) are omitted for clarity.

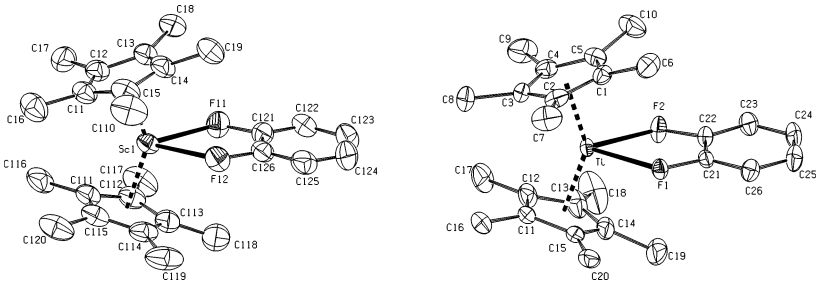

Figure 3. ORTEP representation of the cations of **3a,b** showing 50% probability ellipsoids. The anions and the hydrogen atoms (and the cocrystallized 1,2-difluorobenzene solvent molecule in **3b**) are omitted for clarity.

Table 3. Selected Bond Distances (Å) and Angles(deg) of **2a,b**

	2a	2b
M(*n*1)−Cp*(1)[a,b]	2.1543(12)	2.0093(12)
M(*n*1)−Cp*(2)[c]	2.1475(13)	2.0133(13)
M(*n*1)−F(*n*1)	2.2725(17)	2.151(2)
M(*n*1)−F(12)	2.2884(16)	
C(*n*21)−F(*n*1)	1.408(3)	1.402(3)
C(127)−F(12)	1.414(3)	
Cp*(1)−M(*n*1)−Cp*(2)	141.29(5)	146.53(5)
F(1)−M(*n*1)−F(2)	75.28(6)	
M(*n*1)−F(*n*1)−C(*n*21)	172.21(16)	168.8(2)
M(*n*1)−F(2)−C(127)	165.27(15)	
Σ{angles M(*n*1)}[d]		359.70(9)
∠(Cp*$_2$M,MF$_2$)[e]	89.47(10)	

[a] M = Sc, *n* = 1; M = Ti and V, *n* = 0. [b] Cp*(1) is the centroid of the C(1)−C(5) ring (**2b**) or the C(11)−C(15) ring (**2a,c**). [c] Cp*(2) is the centroid of the C(11)−C(15) ring (**2b**) or the C(111)−C(115) ring (**2a,c**). [d] Σ{angles M(*n*1)} is defined as the sum of the angles around M(*n*1). ∠(Cp*$_2$M,FC$_6$H$_5$) is defined as the angle between the Cp*(1)−M(*n*1)−Cp*(2) and F(11)−M(1)−F(12) planes.

Table 4. Selected Bond Distances (Å) and Angles (deg) of the Cations of **3a,b**

	3a	3b
M(*n*)−Cp*(1)[a,b]	2.1380(18)	2.0452(12)
M(*n*)−Cp*(2)[c]	2.1341(18)	2.0372(12)
M(*n*)−F(*n*1)	2.330(2)	2.3528(13)
M(*n*)−F(*n*2)	2.330(2)	2.2832(15)
C(*n*21)−F(*n*1)	1.389(4)	1.378(3)
C(*n*2*m*)−F(2)[d]	1.396(4)	1.383(2)
Cp*(1)−M(*n*)−Cp*(2)	144.07(7)	144.19(5)
F(*n*1)−M(*n*)−F(*n*2)	68.034(7)	68.58(5)
∠(Cp*$_2$M,MF$_2$)[e]	87.82(8)	87.60(13)
∠(MF$_2$,C$_6$H$_4$F$_2$)[f]	3.76(11)	2.21(8)

[a] M = Sc, *n* = 1; M = Ti, *n* = 0. [b] Cp*(1) is the centroid of the C(*n*1)−C(*n*5) ring. [c] Cp*(2) is the centroid of the C(*n*11)−C(*n*15) ring. [d] M = Sc, *m* = 6; M = Ti, *m* = 2. [e] ∠(Cp*$_2$M,F$_2$C$_6$H$_4$) is defined as the angle between the Cp*(1)−M(1)−Cp*(2) and F(*n*1)−M(*n*)−F(*n*2) planes. [f] ∠(MF$_2$,C$_6$H$_4$F$_2$) is defined as the angle between the F(*n*1)−M(*n*)−F(*n*2) and 1,2-difluorobenzene planes.

from each other (2.3528(13) vs 2.2832(15) Å). The fact that there is no significant difference in the mean M−F bond distance between **3a** and **3b** (although Sc^{3+} is larger than Ti^{3+})[18] suggests that the 1,2-difluorobenzene molecule is more tightly bound in the scandium complex than in the titanium complex. This is in accordance with RIDFT calculations (vide infra). The elongation of the C−F bonds relative to free 1,2-difluorobenzene (M = Sc, 0.040 and 0.047 Å; M = Ti, 0.029 and 0.034 Å) is comparable to that observed for the fluorobenzene adducts (M = Sc, 0.044 and 0.050 Å; M = Ti, 0.038 Å).

Synthesis of Cationic Decamethylmetallocene Cations with the [B(C$_6$F$_5$)$_4$] Anion. Having established that decamethylmetallocene cations can bind neutral fluorobenzenes, we also prepared the cationic metallocenes with the fluorinated "weakly" coordinating [B(C$_6$F$_5$)$_4$] anion. Reaction of Cp*$_2$MMe with [PhNMe$_2$H][B(C$_6$F$_5$)$_4$] in toluene (or, for M = V, in fluorobenzene) resulted in the corresponding ionic complexes [Cp*$_2$M][B(C$_6$F$_5$)$_4$] (**1a′**−**c′**, Scheme 2), which were characterized by single-crystal X-ray diffraction. Initially, in the case of scandium, yellow crystals of the methyl-bridged dimer [(Cp*$_2$Sc)$_2$(μ-Me)][B(C$_6$F$_5$)$_4$] (**4a′**) were obtained, which were characterized by X-ray analysis (see Supporting Information). In the presence of additional [PhNMe$_2$H][B(C$_6$F$_5$)$_4$], dimer **4a′** is converted to two equivalents of [Cp*$_2$Sc(κ^2*F*-C$_6$F$_5$)B(C$_6$F$_5$)$_3$] (**1a′**). The formation of a dimeric compound such as **4a′** was not observed in the case of titanium or vanadium.

The reaction of Cp*$_2$TiMe with [PhNMe$_2$H][B(C$_6$F$_5$)$_4$] performed in fluorobenzene, rather than in toluene, resulted in isolation of either the base-free compound [Cp*$_2$Ti(κ^2*F*-C$_6$F$_5$)B(C$_6$F$_5$)$_3$] (**1b′**) or the fluorobenzene adduct [Cp*$_2$Ti(κ*F*-FC$_6$H$_5$)][B(C$_6$F$_5$)$_4$] (**2b′**), depending on the workup procedure. Simple evaporation of the fluorobenzene and washing with pentane yielded **1b′** as a brown powder. A solution in THF-*d*$_8$ showed ^{1}H NMR resonances of the THF adduct **5b′**, but no liberated fluorobenzene. Layering cyclohexane on top of a fluorobenzene solution of **1b′** yielded green crystals of the fluorobenzene adduct **2b′**, as characterized by X-ray diffraction. Redissolving

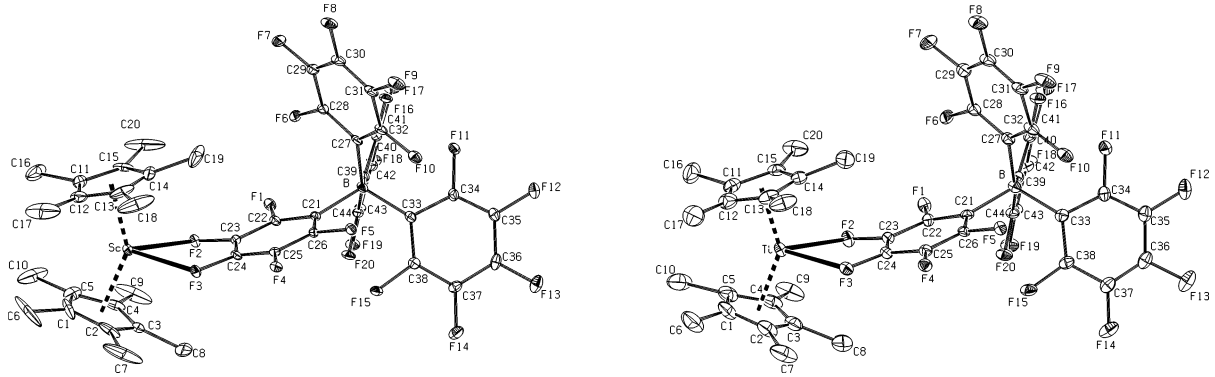

Figure 4. ORTEP representation of **1a′,b′** showing 10% probability ellipsoids. The hydrogen atoms are omitted for clarity.

Scheme 2

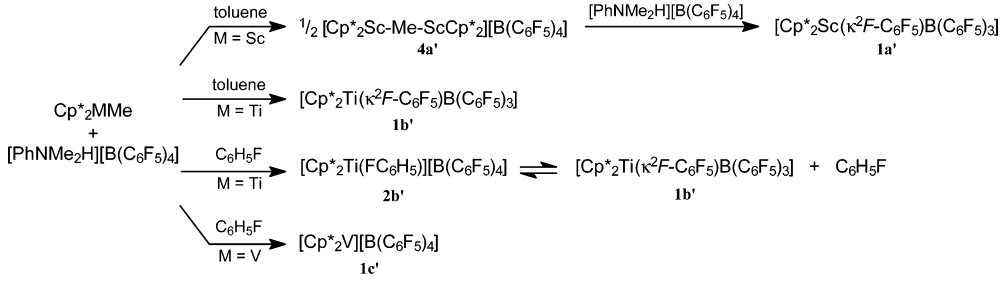

Table 5. Selected Bond Distances (Å) and Angles (deg) of **1a′,b′**

	1a′	**1b′**
M−Cp*(1)[a]	2.115(4)	2.052(7)
M−Cp*(2)[b]	2.138(3)	2.039(5)
M−F(2)	2.341(3)	2.325(5)
M−F(3)	2.392(4)	2.370(5)
C(23)−F(2)	1.377(7)	1.365(10)
C(24)−F(3)	1.383(7)	1.346(10)
Cp*(1)−M−Cp*(2)	144.67(15)	144.9(2)
F(2)−M−F(3)	68.00(12)	67.62(18)
∠(Cp*2M,MF2)[c]	89.3(3)	89.5(5)
∠(MF2,C6F5B)[d]	21.31(15)	20.3(2)

[a] Cp*(1) is the centroid of the C(1)−C(5) ring. [b] Cp*(2) is the centroid of the C(11)−C(15) ring. [c] ∠(Cp*2M,MF2) is defined as the angle between the Cp*(1)−Sc(1)−Cp*(2) and M−F(2)−F(3) planes. [d] ∠(MF2,C6F5B) is defined as the angle between the Cp*(1)−M−Cp*(2) and BC6F5 planes.

crystals of **2b′** in fluorobenzene, followed by evaporation of the solvent and washing with pentane, again yielded the fluorobenzene-free complex **1b′**.

Structure of Decamethylmetallocene Cations with the [B(C6F5)4] Anions. The X-ray structures of [Cp*2M(κ2F-C6F5)B(C6F5)3] (M = Sc, **1a′**; M = Ti, **1b′**) are depicted in Figure 4 (Table 5 contains pertinent bond distances and angles). The anions are coordinated to the metal center in an κ2F-fashion with two adjacent C−F bonds, comparable to the 1,2-difluorobenzene molecules in the adducts **3a,b**. The structures of **1a′,b′** are very similar, with angles between the planes defined by M−F(2)−F(3) and the coordinated C_6F_5 moiety of 21.31(15) and 20.3(2)°, respectively. These angles are significantly larger than those in the 1,2-difluorobenzene adducts **3a,b** (3.76(11) and 2.21(8)°). The M−F bond lengths in **1a′,b′** (M = Sc, 2.341-(3) and 2.392(4) Å; M = Ti, 2.325(5) and 2.370(5) Å) are slightly larger than those in **3a,b** (M = Sc, 2.330(2) and 2.330-(2) Å; M = Ti, 2.3528(13) and 2.2832(15) Å).

An X-ray structure determination of the vanadium analogue **1c′** (see Supporting Information) shows that in this compound there is no direct cation−anion interaction; the cation in **1c′** is virtually identical to that in the tetraphenylborate salt **1c**, with a single agostic interaction of the metal center with a Cp* methyl group. The structure of the cation in the fluorobenzene adduct [Cp*2Ti(FC6H5)][B(C6F5)4] (**2b′**) is very similar to that of [Cp*2-Ti(FC6H5)][BPh4] (**2b**) and will not be discussed in detail here (see Supporting Information).

Synthesis of Cationic Decamethylmetallocene THF Adducts. For comparison with their behavior toward fluoroarenes, the interaction of the decamethylmetallocene cations with the classic Lewis base THF was studied. The reaction of the decamethylmetallocene methyl complexes Cp*2MMe with [PhNMe2H][BPh4] in THF readily generates the THF adducts of the [Cp*2M] cations. Slow diffusion of aliphatic solvents such as pentane or cyclohexane into the THF solutions thus formed afforded yellow crystals of the bis-THF adduct [Cp*2Sc(THF)2]-[BPh4] (**5a**) or green crystals of the mono-THF adducts [Cp*2-Ti(THF)][BPh4] (**5b**) and [Cp*2V(THF)][BPh4] (**5c**).

The ^{1}H NMR spectra of **5a**−**c** in THF-d_8 show resonances for the tetraphenylborate anion. In addition, resonances for the Cp* ligands are observed for diamagnetic **5a** (δ 1.93 ppm) and d^1 paramagnetic **5b** (δ 11.7 ppm with $\Delta\nu_{1/2}$ = 402 Hz). For the d^2 compound **5c**, no resonance for the Cp* ligand could be observed in the chemical shift range −150 to 150 ppm. This indicates that the d^2 center in **5c** has an $S = 1$ configuration, as is usual for electronically unsaturated V(III) compounds.[15,25]

Structure of the Cationic Decamethylmetallocene THF Adducts. The three THF adducts **5a**−**c** were characterized by single-crystal X-ray diffraction (Figure 5, pertinent geometric data in Table 6). The structure of the scandium bis(THF-d_8) adduct, **5a-*d*16** (crystallized from THF-d_8/pentane), is very similar to that of the known lanthanide species [Cp*2Ln(THF)2]-

(25) (a) Nieman, J.; Teuben, J. H.; Huffman, J. C.; Caulton, K. G. *J. Organomet. Chem.* **1983**, *255*, 193. (b) Hessen, B.; Meetsma, A.; Teuben, J. H. *J. Am. Chem. Soc.* **1989**, *111*, 5977. (c) Choukroun, R.; Couziech, B.; Pan, C.; Dahan, F.; Cassoux, P. *Organometallics* **1995**, *14*, 4471.

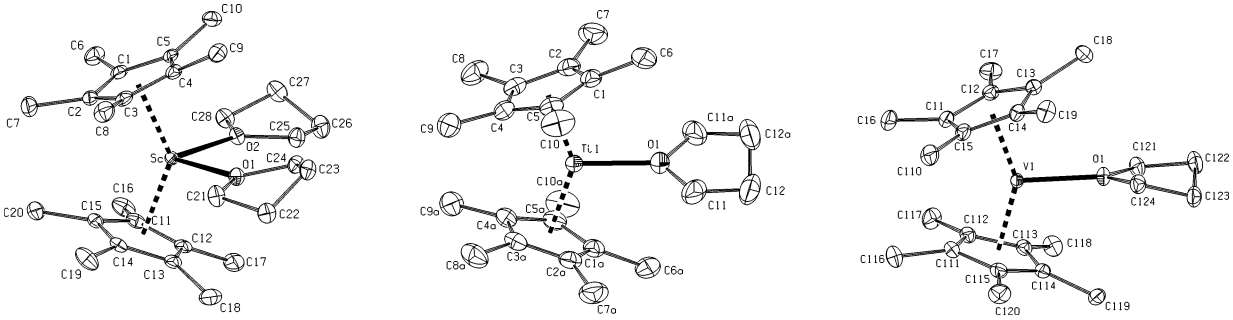

Figure 5. ORTEP representation of the cations of **5a-d_{16}** and **5b,c** showing 50% probability ellipsoids. The anions and hydrogen atoms (and the deuterium atoms in **5a-d_{16}**) are omitted for clarity.

Table 6. Selected Bond Distances (Å) and Angles (deg) or **5a-d_{16}** and **5b,c**

	5a-d_{16}	5b	5c
M(n)−Cp*(1)[a,b]	2.2228(9)	2.0479(14)	1.9810(6)
M(n)−Cp*(2)[c]	2.2302(10)		1.9907(6)
M(n)−O(1)	2.2964(14)	2.116(3)	2.1189(8)
M(n)−O(2)	2.2652(14)		
Cp*(1)−M(n)−Cp*(2)	137.21(4)	142.11(6)	146.51(2)
O(1)−M(n)−O(2)	91.59(5)		
Σ{angles O(1)}[d]	358.9(2)	360.0(4)	359.98(13)
Σ{angles O(2)}[e]	360.0(2)		
Σ{angles M(n)}[f]		360.01(8)	360.00(5)
∠(Cp*$_2$M,MOCC)[g]		73.11(17)	80.43(7)
∠(Cp*$_2$M,OMO)[h]	89.69(15)		

[a] M = Sc, n = 0; M = Ti and V, n = 1. [b] Cp*(1) is the centroid of the C(n1)−C(5) ring (M = Sc and Ti) or the C(11)−C(15) ring (M = V). [c] Cp*(2) is the centroid of the C(11)−C(15) ring (M = Sc and Ti) or the C(111)−C(115) ring (M = V). [d] Σ{angles O(1)} is defined as the sum of the angles around atom O(1). [e] Σ{angles O(2)} is defined as the sum of the angles around atom O(2). [f] Σ{angles M(n)} is defined as the sum of the angles around atom M(n). [g] ∠(Cp*$_2$M,MOCC) is the angle between the Cp*(1)−M(1)−Cp*(2) and Ti(1)−O(1)−C(11)−C(11a) or V(1)−O(1)−C(121)−C(124) planes. [h] ∠(Cp*$_2$M,OMO) is the angle between the Cp*(1)−M(1)−Cp*(2) and O(1)−M(1)−O(2) planes.

$[BPh_4]$ (Ln = Sm[26] and Yb[27]). The two Sc−O distances in **5a-d_{16}** differ slightly (by 0.03 Å), and the O−Sc−O angle of 91.59(1)° is noticeably larger than the F−Sc−F angle of 75.28(6)° in the bis-fluorobenzene adduct **2a**.

The asymmetric unit of the titanium mono-THF adduct **5b** contains two independent $[Cp^*_2Ti(THF)]$ cations, each located on a crystallographic C_2 axis, that are virtually identical. Data of only one of these are included in Table 6. Only one THF molecule is bound to the metal center, contrasting with the bis-THF adduct observed for the parent metallocene cation $[Cp_2Ti(THF)_2]^+$. As expected for a complex with a lower coordination number, the Ti(1)−O(1) bond distance in **5b** of 2.116(3) Å is shorter than those in $[Cp_2Ti(THF)_2]^+$ (2.19−2.24 Å).[28] The THF adducts **5a,b** have a geometry similar to those of the corresponding fluorobenzene adducts **2a,b** with slightly smaller Cp*−M−Cp* angles (M = Sc, 137.21(4) vs 141.29(5)°; M = Ti, 142.11(6) vs 146.53(5)°).

The geometry of the cationic vanadium mono-THF adduct in **5c** closely resembles that of the titanium analogue. Differences in M−Cp* bonding can be accounted for by the relative size of the Ti^{3+} and V^{3+} ions (effective ionic radii are 0.670 and 0.640 Å, respectively).[18] In that respect, the V(1)−O(1) bond distance in **5c** (2.1189(8) Å) is relatively long compared to the Ti−O bond distance in **5b** (2.116(3) Å), suggesting that the THF molecule is more tightly bound in the case of titanium (vide infra).

Computational Studies. The base-free decamethylmetallocene cations, their THF, fluorobenzene, and 1,2-difluorobenzene adducts were studied by DFT calculations (RI-bp86/SV(P); see Experimental Section for details and Supporting Information for complete results). Also included were the parent metallocene cations, $[Cp_2M]^+$, and their corresponding adducts. Results are summarized in Table 7 and are graphically represented in Figure 6. The energies are relative to the base-free metallocene cations and do not include zero-point energies or thermal corrections, and the anions have been omitted.

The optimized structures of all adducts adopt a bent-metallocene geometry and are in reasonable agreement with the X-ray structures described above (when available), the main difference being the M−X bond lengths, which are longer in the case of the calculated structures by 0.08−0.13 Å. The energy associated with the shortening of the M−X bond distances to the values found in the X-ray structures, however, is small (<1.5 kcal/mol, see Supporting Information). We therefore think that this shortening of the bond lengths is a result of crystal packing forces, reducing the distance between the cation and anion, hence increasing Coulombic stabilization. Similar to those found in the X-ray structures, the C−F bond lengths in the calculated structures of the fluorobenzene adducts are longer than those in the free fluoroaromatics. The M−F−C angles in the calculated structures of the decamethylmetallocene fluorobenzene adducts are close to 180° and are thus similar to those found in the X-ray analyses. In the case of the cationic $[Cp_2M]$ monofluorobenzene adducts, this angle is much smaller (139.66−149.63 °).

The base-free metallocene cations were studied not only as a reference to the adducts described here but also to investigate the nature of the agostic interactions observed in the base-free metallocene cations **1b,c**. For $[Cp^*_2Sc]^+$, the similarity between the observed and calculated structures indicates that the close contact between the cation and the BPh_4^- anion observed in the solid state does not represent a strong chemical interaction. For the titanocene cation, the optimized structure shows no agostic interactions, but a structure in which these interactions are present is just 2.42 kcal/mol higher in energy. Furthermore, in the case of the decamethylvanadocene cation, two local

(26) Evans, W. J.; Ulibarri, T. A.; Chamberlain, L. R.; Ziller, J. W.; Alvares, D. *Organometallics* **1990**, *9*, 2124.
(27) Schumann, H.; Winterfeld, J.; Keitsch, M. R.; Herrmann, K.; Demtschuk, J. *Z. Anorg. Allg. Chem.* **1996**, *622*, 1457.
(28) (a) Merola, J. S.; Campo, K. S.; Gentile, R. A.; Modrick, M. A. *Inorg. Chim. Acta* **1989**, *195*, 87. (b) Ohff, A.; Kempe, R.; Baumann, W.; Rosenthal, U. *J. Organomet. Chem.* **1996**, *520*, 241. (c) Ahlers, W.; Temme. B.; Erker, G.; Fröhlich, R.; Zippel, F. *Organometallics* **1997**, *16*, 1440. (d) Plecnik, C. E.; Liu, F. C.; Liu, S. M.; Liu, J. P.; Meyers, E. A.; Shore, S. G. *Organometallics* **2001**, *20*, 3599.

Table 7. RIDFT/bp86 Results for $[Cp_2ML_n]^+$ and $[Cp^*_2ML_n]^+$ Systems (M = Sc, Ti, and V; L = C_6H_5F, 1,2-$C_6H_4F_2$, and THF)[a]

	E_{rel}[b] (kcal/mol)	M–X (Å)	C–X (Å)	M–X–C (deg)
$[Cp_2Sc(FC_6H_5)]^+$	−21.68	2.22	1.42	142.15
$[Cp_2Sc(FC_6H_5)_2]^+$	−33.79	2.27, 2.28	1.41, 1.41	163.79, 158.55
$[Cp_2Sc(F_2C_6H_5)]^+$	−28.35	2.37, 2.37	1.39, 1.39	
$[Cp_2Sc(THF)]^+$	−36.50	2.20		
$[Cp_2Sc(THF)_2]^+$	−42.73	2.27, 2.28		
$[Cp_2Ti(FC_6H_5)]^+$	−19.85	2.18	1.42	142.22
$[Cp_2Ti(FC_6H_5)_2]^+$	−28.14	2.32, 2.32	1.40, 1.40	155.99, 151.44
$[Cp_2Ti(F_2C_6H_5)]^+$	−26.53	2.34, 2.34	1.38, 1.38	
$[Cp_2Ti(THF)]^+$	−35.14	2.15		
$[Cp_2Ti(THF)_2]^+$	−51.17	2.29, 2.27		
$[Cp_2V(FC_6H_5)]^+$	−18.10	2.22	1.41	139.66
$[Cp_2V(FC_6H_5)_2]^+$	−19.90	2.25, 3.26	1.41, 1.37	142.67, 149.63
$[Cp_2V(F_2C_6H_5)]^+$	−18.92	2.26, 3.00	1.39, 1.35	
$[Cp_2V(THF)]^+$	−35.12	2.12		
$[Cp_2V(THF)_2]^+$	−24.61	2.18, 2.22		
$[Cp^*_2Sc(FC_6H_5)]^+$	−14.44	2.29	1.41	165.71
$[Cp^*_2Sc(FC_6H_5)_2]^+$	−20.54	2.39, 2.40	1.40, 1.40	168.88, 167.54
$[Cp^*_2Sc(F_2C_6H_5)]^+$	−17.17	2.45, 2.45	1.38, 1.38	
$[Cp^*_2Sc(THF)]^+$	−23.05	2.29		
$[Cp^*_2Sc(THF)_2]^+$	−27.83	2.38, 2.36		
$[Cp^*_2Ti]^+$	0.00		1.12, 1.13	
$[Cp^*_2Ti(FC_6H_5)]^+$	−11.58	2.27	1.41	164.61
$[Cp^*_2Ti(FC_6H_5)_2]^+$	−13.94	2.47, 2.51	1.39, 1.39	165.40, 164.73
$[Cp^*_2Ti(F_2C_6H_5)]^+$	−15.37	2.40, 2.40	1.38, 1.38	
$[Cp^*_2Ti(THF)]^+$	−19.19	2.25		
$[Cp^*_2Ti(THF)_2]^+$	−15.73	2.37, 2.48		
$[Cp^*_2V]^+$	0.28			
$[Cp^*_2V]^+$ (agostic)	0.00	2.10	1.16	
$[Cp^*_2V(FC_6H_5)]^+$	−6.55	2.33	1.40	163.28
$[Cp^*_2V(FC_6H_5)_2]^+$	−9.28	2.37, 4.00	1.40, 1.37	165.24, 152.76
$[Cp^*_2V(F_2C_6H_5)]^+$	−6.44	2.39, 3.19	1.38, 1.35	
$[Cp^*_2V(THF)]^+$	−13.79	2.23		

[a] Energies (kcal/mol) are for the reaction $Cp'_2M + 2L \rightarrow Cp'_2ML_n + (2-n)L$. Distances are measured in Å and angles are measured in deg. X denotes the ligand heteroatom or (for the agostic species) the Cp*H atom. [b] Relative to the base-free metallocene cation.

minima are found, one of which does show such an agostic interaction (the energy difference between the two structures is 0.28 kcal/mol, with the agostic structure being the lowest in energy).

The calculations corroborate the observations that the scandocene cation prefers the formation of a bis-THF adduct, in the case of both the $[Cp_2Sc]$ and the $[Cp^*_2Sc]$ cation. They furthermore agree with the observation that the parent titanocene cation binds two molecules of THF, whereas a mono-THF adduct is obtained in the case of the decamethyltitanocene cation, and with the fact that the vanadocene cation binds only one molecule of THF irrespective of the substitution pattern of the cyclopentadienyl ligand (in fact, the second molecule of THF dissociates when trying to optimize the structure of the $[Cp^*_2V(THF)_2]$ cation).

In the case of fluorobenzene, the binding of one or two molecules of fluorobenzene is enthalpically favorable in the case of all metallocene cations considered. Nevertheless, for the compounds that were not accessible in the experiments described above, the binding energy is very low (lower than the expected loss of entropy on complex formation, which is estimated at 10 kcal/mol). For example, the energy associated with the binding of fluorobenzene to the decamethylvanadocene cation is only 6.55 kcal/mol.

The binding energies decrease with an increasing number of unpaired electrons, except for the mono-THF adducts of the $[Cp_2M]$ cations. This parallels the relative M−X bond lengths in the X-ray structures of the 1,2-difluorobenzene adducts **3a,b** and of the THF adducts **5b,c**. Furthermore, the binding energies of fluorobenzene and 1,2-difluorobenzene are smaller than that of THF, which is a much better σ donor.

Discussion

Considering the molecular orbital (MO) scheme of the bent-metallocene fragment,[29] there are three orbitals suitable for the binding of additional substrates, with C_{2v} symmetry labels $1a_1$, b_2, and $2a_1$ in order of increasing energy. For the d^0 metal ion Sc(III), all three orbitals are, in principle, available for the binding of additional ligands. For the d^1 ion Ti(III) and the d^2 ($S = 1$) ion V(III), orbitals are occupied by unpaired electron(s), leaving two (Ti) or one (V) free valence orbitals, respectively.

In addition to the number of available valence orbitals, the coordination chemistry of the $[Cp^*_2M]$ cations is determined by the accessibility of the metal center. For $[Cp^*_2Ti]^+$, the space in the wedge between the ligands only allows the binding of a single THF molecule, whereas the electronic configuration would allow the binding of two THF molecules, as seen in the unsubstituted metallocene cation $[Cp_2Ti(THF)_2]^+$.[28] The d^2 $S = 1$ $[Cp^*_2V]$ cation can bind only one molecule of THF, irrespective of the substituents on the cyclopentadienyl ligand.[30] The vanadocene cation can only accommodate two additional ligands in the case of a strong field ligand such as CO. In that case, the binding is accompanied by spin pairing, as seen in the bis-CO adducts $[Cp_2V(CO)_2][Co(CO)_4]$ and $[Cp_2V(CO)_2][BPh_4]$.[31] From the DFT calculations, it can clearly be seen that in the decamethylmetallocene cations the THF binding energies have a significant steric component; in the $[Cp_2M(THF)]$ cations, the THF molecule is bound equally strong, irrespective of the metal center, whereas the THF binding energy in the corresponding $[Cp^*_2M(THF)]$ cations differs for the three metals corresponding to the relative accessibility of the metal center (Sc > Ti > V).

The interplay of steric and electronic effects is also seen in the structures of the base-free $[Cp^*_2M][BPh_4]$ compounds. Whereas for scandium the metallocene wedge is sufficiently open to allow interaction with the anion, the titanium and vanadium cations cannot accommodate this. Instead, these metallocene cations adopt (at least in the solid state) structures with agostic interactions with Cp*−Me groups. It is presently unclear whether these observed distortions are due to an increase in Coulombic lattice energy (e.g., by allowing the anion to approach the cation more closely) or due to true electronic stabilization by these intramolecular interactions. The DFT calculations on the isolated cations indicate no (Ti) or very small (V) stabilizations upon distortion. Nevertheless, the fact that the number of agostic interactions corresponds to the number of free valence orbitals on the metal center (two for Ti, one for V) suggests that these interactions are at least *enabled* by the electronic configuration of the metal. Even though agostic C−H···M interactions are well-known in early transition-metal chemistry,[32] intramolecular interactions with methyl substituted Cp ligands are, to our knowledge, unprecedented.

(29) (a) Lauher, J. W.; Hoffmann, R. *J. Am. Chem. Soc.* **1976**, *98*, 1729. (b) Green, J. C. *Chem. Soc. Rev.* **1998**, *27*, 263.
(30) Choukroun, R.; Douziech, B.; Pan, C.; Dahan, F.; Cassoux, P. *Organometallics* **1995**, *14*, 4471.
(31) (a) Calderazzo, F.; Bacciarelli, S. *Inorg. Chem.* **1963**, *2*, 721. (b) Calderazzo, F.; Ferri, I.; Pampaloni, G. *Organometallics* **1999**, *18*, 2452.

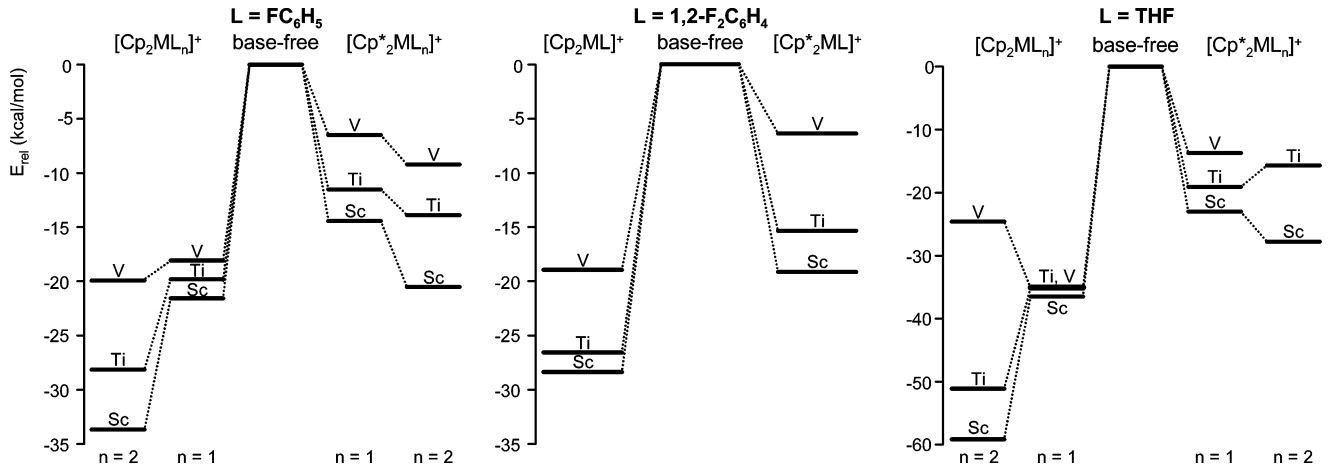

Figure 6. Relative energies of C_6H_5F, $C_6H_4F_2$, and THF adducts of metallocenium cations. Note the different vertical scale for the THF adducts.

Reaction of the base-free decamethylmetallocene cations with fluorobenzenes resulted in the isolation of the first κF-fluorobenzene and $\kappa^2 F$-1,2-difluorobenzene adducts of transition metals. There are a limited number of κX-halobenzene (X = Cl, Br, and I)[33] and $\kappa^2 I$-1,2-diiodobenzene adducts known to date.[34] In the κX-halobenzene adducts, the M−X−C angle (95.361−116.406°) is generally much smaller than the ca. 180° observed in our κF-fluorobenzene adducts. To our knowledge, the only other example of a halobenzene adduct with a linear M−X−C bond is the lithium fluorobenzene adduct $Li_2[\mu\text{-}N(SiMe_3)_2]_2(C_6H_5F)$.[35] It appears that the metal−fluorobenzene interaction in the cationic metallocene adducts described here is also predominantly electrostatic in nature. The calculated ligand binding energies corroborate the poor σ donor character of the fluorine atom compared to that of the oxygen atom of THF. π Back-bonding to the fluorobenzene ligand (necessarily absent in the case of the d^0 metal ion Sc^{3+}) is negligible in the case of the titanium and (hypothetical) vanadium complexes; the spin density in these complexes is mainly located in metal-centered orbitals (see Supporting Information).

The metal−fluoroarene interactions in the $\kappa^2 F$-1,2-difluorobenzene adducts and the $[Cp^*_2Ti(\kappa^2 F\text{-}C_6F_5)B(C_6F_5)_3]$ complexes are comparable, though the M−F bond distances in the $B(C_6F_5)_4$ adducts are slightly larger than those in the corresponding 1,2-difluorobenzene adducts. As the Cp* ligands have a large degree of freedom, as seen by their rotational disorder in the crystal structure, it is unlikely that these longer M−F bonds are the result of steric repulsion of the Cp* ligands with the C_6F_5 groups of the anion. Instead, it might be that, due to the strong electron-withdrawing nature of all other fluorine substituents in the anion, the amount of negative charge at the two coordinating fluorines is actually *smaller* than in the difluorobenzene complexes. The relative weakness of the metal−$B(C_6F_5)_4$ interaction is also underlined by the observation of an equilibrium between the contact ion pair $[Cp^*_2Ti(\kappa^2 F\text{-}C_6F_5)B(C_6F_5)_3]$ and the fluorobenzene adduct $[Cp^*_2Ti(\kappa F\text{-}FC_6H_5)][B(C_6F_5)_4]$ in fluorobenzene solution.

Conclusions

The decamethylmetallocene cations $[Cp^*_2M]^+$ (M = Sc, Ti, and V), with d^0−d^2 metal electronic configurations, were generated for use as scaffolds to probe the interactions of the cationic metal center with the C−F bonds of fluoroarenes. The coordination chemistry of the metal centers in these species is governed by the number of free valence orbitals and by the spatial accessibility of the metal center through the wedge formed by the Cp* ligands. The balance of these factors is illustrated, for example, by the observed stoichiometries of complexes with Lewis bases such as THF, but also by the structures of the base-free species. For the largest metal, scandium, $[Cp^*_2M][BPh_4]$ forms a contact ion pair in the solid state, whereas for the smaller titanium and vanadium metals, the anion cannot be accommodated in the metallocene cleft. Instead, the cations in these compounds adopt unprecendented distorted metallocene structures with agostic C−H···M interactions to one (V) or two (Ti) of the Cp* methyl groups. These substantial deformations seem to be associated with surprisingly small energy changes.

The decamethylmetallocene cations of scandium and titanium react with fluorobenzenes to give isolable, fluorine-bound adducts $[Cp^*_2M(\kappa F\text{-}FC_6H_5)_n][BPh_4]$ (M = Sc, n = 2; M = Ti, n = 1) and $[Cp^*_2M(\kappa^2 F\text{-}1,2\text{-}F_2C_6H_4)][BPh_4]$, whereas for the smallest and least electropositive metal vanadium, the interaction with fluoroarenes is too weak to allow isolation of adducts. The bonding of the fluoroarene molecules in these complexes appears to be governed mainly by electrostatics. In view of these observations, it comes as no surprise that the perfluorinated $[B(C_6F_5)_4]$ anion coordinates to the Sc and Ti cations in much the same way as 1,2-difluorobenzene. Nevertheless, it is remarkable that neutral fluorobenzene can compete with the $[B(C_6F_5)_4]$ anion for bonding to the metal center in the Ti system. Apparently, the 20 fluoro atoms in the anion can

(32) (a) Dawoodi, Z.; Green, M. L. H.; Mtetwa, V. S. B.; Prout, K. *Chem. Commun.* **1982**, 802. (b) Jordan, R. F.; Bradley, P. K.; Baenziger, N. C.; LaPointe, R. E. *J. Am. Chem. Soc.* **1990**, *112*, 1289. (c) Hyla-Krypsin, I.; Gleiter, R.; Kruger, C.; Zwettler, R.; Erker, G. *Organometallics* **1990**, *9*, 517. (d) Bochmann, M.; Lancaster, S. J.; Hursthouse, M. B.; Abdul Malik, K. M. *Organometallics* **1994**, *13*, 2235. (e) Pindado, G. J.; Thornton-Pett, M.; Bouwkamp, M. W.; Meetsma, A.; Hessen, B.; Bochmann, M. *Angew. Chem., Int. Ed.* **1997**, *36*, 2358. (f) Nakamura, H.; Nakayama, Y.; Yasuda, H.; Maruo, T.; Kanehisa, N.; Kai, Y. *Organometallics* **2000**, *19*, 5392. (g) Schmitt, O.; Wolmershäuser, G.; Sitzmann, H. *Eur. J. Inorg. Chem.* **2003**, 3105.
(33) (a) Kullawiek, R. J.; Faller, J. W.; Crabtree, R. H. *Organometallics* **1990**, *9*, 745. (b) Butts, M. D.; Scott, B. L.; Kubas, G. J. *J. Am. Chem. Soc.* **1996**, *118*, 11831. (c) Powell, J.; Horvath, M. J.; Lough, A. *J. Chem. Soc., Dalton Trans.* **1996**, 1669. (d) Wu, F.; Dash, A. K.; Jordan, R. F. *J. Am. Chem. Soc.* **2004**, *126*, 15360.
(34) (a) Crabtree, R. H.; Faller, J. W.; Mellea, M. F.; Quirck, J. M. *Organometallics* **1982**, *1*, 1361. (b) Powell, J.; Lough, A.; Saeed, T. *J. Chem. Soc., Dalton Trans.* **1997**, 4137.
(35) Williard, P. G.; Liu, Q. Y. *J. Org. Chem.* **1994**, *59*, 1596.

dissipate the negative charge sufficiently to allow this competition, a tribute to the weakly nucleophilic nature of this anion. An interesting aside is the observation that, despite its weak nucleophilicity, the $[B(C_6F_5)_4]$ anion shows a stronger interaction with the Ti center than the $[BPh_4]$ anion that is usually considered to be more strongly interacting. In this case, this is probably dictated by geometric factors; the most favorable coordination mode of the $[BPh_4]$ anion (through one of the CH═CH moieties of the phenyl group) is not accessible because of the steric demand of the two Cp* ligands bound to the relatively small Ti center.

Experimental Section

General Considerations. All reactions and manipulations of air- and moisture-sensitive compounds were performed under a nitrogen atmosphere using standard Schlenk, vacuum line, and glovebox techniques. Reagents were purchased from commercial suppliers and used as received, unless stated otherwise. Deuterated solvents were dried over Na/K alloy prior to use or degassed and stored over molecular sieves (4 Å) (fluorobenzene-d_5). Other solvents were dried by percolation over columns of aluminum oxide (THF and toluene), R3-11 supported Cu-based oxygen scavengers (THF, pentane and toluene), and molecular sieves (pentane and toluene) or by distillation from Na/K alloy (cyclohexane). Fluorobenzene and 1,2-difluorobenzene were dried and stored over molecular sieves. The compounds Cp^*_2ScMe,[13] Cp^*_2TiMe,[14] Cp^*_2VMe,[15] and $[PhNMe_2H][BPh_4]$[16] were prepared according to literature procedures. ^1H and ^{19}F NMR spectra were recorded on a Varian Unity 500 or Varian Gemini 200 spectrometer. Chemical shifts are reported in ppm and are referenced to residual solvent resonances. IR spectra were recorded on a Mattson 4020 Galaxy Fourier transform infrared (FT-IR) spectrophotometer. The elemental analyses were performed by the Microanalytical Department of the University of Groningen or by H. Kolbe, Mikroanalytisches Laboratorium, Mülheim an der Ruhr. In the case of the analyses performed at the University of Groningen, each value is the average of two independent determinations. Some of these analyses show low, but reproducible, carbon values. This is a common observation for organometallic complexes with a high carbon content and is associated with the formation of inert carbide species. In all cases, V_2O_5 was added to the samples to reduce the formation of such species. The analysis performed under different conditions by Kolbe does not suffer from these low carbon values. The values reported in this case are single measurements. An extended experimental section including alternative methods of preparation, Toepler pump experiments, and a detailed description of the X-ray diffraction studies can be found in the Supporting Information.

$[Cp^*_2Sc][BPh_4]$ (1a). Toluene (5 mL) was added to a mixture of 507 mg (1.5 mmol) of Cp^*_2ScMe and 627 mg (1.5 mmol) of $[PhNMe_2H][BPh_4]$. After 1 h, the solvent was evaporated and the resulting yellow solid was washed with pentane (3 × 5 mL), affording 631 mg (1.0 mmol, 67%) of $[Cp^*_2Sc][BPh_4]$. Anal. Calcd for $C_{44}H_{50}BSc$: C, 83.39; H, 7.95. Found: C, 83.16; H, 7.95.[36] Compound **1a** is slightly soluble in C_6D_6, but insufficiently to record ^1H and ^{13}C NMR spectra.

$[Cp^*_2Ti][BPh_4]$ (1b). To a mixture of 0.75 g (2.2 mmol) of Cp^*_2TiMe and 0.95 g (2.2 mmol) of $[PhNMe_2H][BPh_4]$ was added 40 mL of toluene at −30 °C. Gas evolution was observed as the solution was gradually warmed to room temperature. After 1 h, the toluene was removed at reduced pressure and the crystalline solid was washed with pentane (3 × 20 mL). Drying the product in a vacuum afforded 1.2 g (1.8 mmol, 86%) of $[Cp^*_2Ti][BPh_4]$ as red-brown crystals, suitable for single-crystal X-ray diffraction. Anal. Calcd for $C_{44}H_{50}BTi$: C, 82.89; H, 7.90. Found: C, 79.62; H, 8.06.[37]

$[Cp^*_2V][BPh_4]$ (1c). To a mixture of 201 mg (0.60 mmol) of Cp^*_2VMe and 242 mg (0.59 mmol) of $[PhNMe_2H][BPh_4]$ was added 5 mL of toluene. After 1 h, the toluene was evaporated at reduced pressure and the product was washed with pentane (3 × 3 mL). Evaporation of the volatiles at reduced pressure yielded 263 mg (0.42 mmol, 71%) of $[Cp^*_2V][BPh_4]$ as a brown powder. Recrystallization of the compound from 1,2-difluorobenzenze/cyclohexane afforded reddish crystals that were used in an X-ray diffraction study. Crystals thus obtained were also submitted for elemental analysis. Anal. Calcd for $C_{44}H_{50}BV$: C, 82.49; H, 7.87. Found: C, 80.86; H, 7.86.[37]

$[Cp^*_2Sc(\kappa F\text{-}FC_6H_5)_2][BPh_4]$ (2a). $[Cp^*_2Sc][BPh_4]$ (25.9 mg, 41 μmol) was dissolved in 1 mL of fluorobenzene. Slow evaporation of the solvent at reduced pressure afforded 8.9 mg (9 μmol, 21%) of yellow crystals of $[Cp^*_2Sc(FC_6H_5)_2][BPh_4]\cdot 2C_6H_5F$. Anal. Calcd for $C_{56}H_{60}BF_2Sc\cdot 2C_6H_5F$: C, 79.85; H, 6.93. Found: C, 80.22; H, 7.86.[36]

$[Cp^*_2Ti(\kappa F\text{-}FC_6H_5)][BPh_4]$ (2b). Fluorobenzene (40 mL) was added to a frozen mixture of 660 mg (1.98 mmol) of Cp^*_2TiMe and 874 mg (1.98 mmol) of $[PhNMe_2H][BPh_4]$. The frozen mixture was allowed to warm to ambient temperature, and the reaction mixture was stirred. The color darkened while gas evolution was observed. After 3 h, the solution was decanted and concentrated. Crystallization by slow diffusion of pentane into the fluorobenzene solution yielded 869 mg (1.04 mmol, 53%) of $[Cp^*_2Ti(FC_6H_5)][BPh_4](C_6H_5F)$. Anal. Calcd for $C_{50}H_{55}BFTi\cdot C_6H_5F$: C, 81.06; H, 7.29; Ti, 5.77. Found: C, 80.36; H, 7.40; Ti, 5.62.[37]

$[Cp^*_2Sc(\kappa^2F\text{-}F_2C_6H_4)][BPh_4]$ (3a). 1,2-Difluorobenzene (0.5 mL) was added to 24.8 mg (39 μmol) of $[Cp^*_2Sc][BPh_4]$. On top of the solution, 3 mL of cyclohexane was layered carefully. Slow mixing of the two layers resulted in the precipitation of 12.9 mg (17 μmol, 44%) of $[Cp^*_2Sc(F_2C_6H_4)][BPh_4]$. Anal. Calcd for $C_{50}H_{54}BF_2Sc$: C, 80.30; H, 7.28. Found: C, 80.03; H, 7.11.[36]

$[Cp^*_2Ti(\kappa^2F\text{-}F_2C_6H_4)][BPh_4]$ (3b). $[Cp^*_2Ti][BPh_4]$ (54.2 mg, 85 μmol) was dissolved in 0.5 mL of 1,2-difluorobenzene. The green solution was layered with 2.5 mL of cyclohexane. Slow diffusion of the cyclohexane into the 1,2-difluorobenzene solution afforded 58.6 mg (68 μmol, 80%) of blue-green crystals of $[Cp^*_2Ti(1,2\text{-}F_2C_6H_5)][BPh_4]\cdot(C_6H_4F_2)$. The ^1H NMR spectrum of the compound in THF-d_8 was identical to that of the mono-THF adduct **5b** and showed resonances for 1,2-difluorobenzene. Anal. Calcd for $C_{50}H_{54}BF_2Ti\cdot C_6H_4F_2$: C, 77.69; H, 6.75; Ti, 5.33. Found: C, 77.68; H, 6.85; Ti, 5.53.[36] In a separate experiment, 34 mg (55 μmol) of $[Cp^*_2Ti][BPh_4]$ was dissolved in 0.5 mL of 1,2-difluorobenzene. From this solution, 40.2 mg (46 μmol, 84%) of blue-green crystals of $[Cp^*_2Ti(1,2\text{-}F_2C_6H_5)][BPh_4]\cdot(C_6H_4F_2)$ were obtained after slow diffusion of cyclohexane into the solution.

$[Cp^*_2Sc(\kappa^2F\text{-}C_6F_5)B(C_6F_5)_3]$ (1a′). Toluene (1 mL) was added to a mixture of 30.6 mg (93 μmol) of Cp^*_2ScMe and 73.0 mg (91 μmol) of $[PhNMe_2H][B(C_6F_5)_4]$. The resulting solution was layered with cyclohexane resulting in a brownish, oily precipitate. Upon standing for one week, the compound crystallized to yield 55.3 mg (56 μmol, 62%) of $[Cp^*_2Sc][B(C_6F_5)_4]$ after decanting of the toluene solvent and washing with pentane (2 × 2 mL). Anal. Calcd for $C_{44}H_{30}BF_{20}Sc$: C, 53.19; H, 3.04. Found: C, 53.16; H, 3.32.[37]

$[Cp^*_2Ti(\kappa^2F\text{-}C_6F_5)B(C_6F_5)_3]$ (1b′) from Cp^*_2TiMe and $[PhNMe_2H][B(C_6F_5)_4]$. To a mixture that was frozen in liquid nitrogen of 122 mg (0.37 mmol) of Cp^*_2TiMe and 320 mg (0.35 mmol) of $[PhNMe_2H][B(C_6F_5)_4]$ was added 10 mL of fluorobenzene. The reaction mixture was stirred for 1 h, resulting in a green solution. The solvent was removed in a vacuum, and the resulting green oil was washed 5 times with 10 mL of pentane. After drying in a vacuum, this afforded 0.30 g (0.3 mmol, 86%) of $[Cp^*_2Ti][B(C_6F_5)_4]$. The ^1H and ^{19}F NMR spectra of the compound in THF-d_8 show resonances for the THF adduct **5b′** and for a diamagnetic impurity with a resonance at 2.05 ppm (17% assuming the impurity involves a $[Cp^*_2M]$ fragment). Hence, no satisfactory elemental analysis could be obtained.

$[Cp^*_2Ti(\kappa^2F\text{-}C_6F_5)B(C_6F_5)_3]$ (1b′) from Cp^*_2TiMe and $[(C_nH_{2n+2})_2NMeH][B(C_6F_5)_4]$ ($n = 16-18$). Cyclohexane (0.5 mL) and 32.6 mg

(36) Measured at the Microanalytical Department of H. Kolbe (Mülheim an der Ruhr).
(37) Measured at the Microanalytical Department of the University of Groningen.

(98 μmol) of Cp^*_2TiMe in another 0.5 mL of cyclohexane was layered on top of 1.04 g of a 10.8 wt % ISOPAR solution (94 μmol) of $[(C_nH_{2n+2})_2NMeH][B(C_6F_5)_4]$ ($n = 16-18$). The two layers mixed slowly, resulting in a brown, oily precipitate. Greenish-brown crystals that were suitable for X-ray analysis precipitated overnight. Washing of the crystals with pentane (2 mL) resulted in 75 mg (75 μmol, 77%) of $[Cp^*_2Ti][B(C_6F_5)_4]$. The ^1H and ^{19}F NMR spectra of the compound in THF-d_8 are similar to those of **5b′**. Anal. Calcd for $C_{44}H_{30}BF_{20}Ti$: C, 52.99; H, 3.03. Found: C, 50.75; H, 3.35.[37]

$[Cp^*_2Ti(FC_6H_5)][B(C_6F_5)_4]$ (2b′). To a mixture of 33.0 mg (99 μmol) of Cp^*_2TiMe and 75.6 mg (94 μmol) of $[PhNMe_2H][B(C_6F_5)_4]$ was added 1 mL of fluorobenzene. Slow diffusion of 3 mL of cyclohexane into the fluorobenzene resulted in 79.3 mg (80 μmol, 80%) of green crystals. The compound was recrystallized from fluorobenzene/cyclohexane to afford crystals that were suitable for a single-crystal X-ray analysis. Crystals thus obtained were also submitted for elemental analysis. Anal. Calcd for $C_{50}H_{35}BF_{21}Ti$: C, 54.92; H, 3.23. Found: C, 53.84; H, 3.34. [37]

$[Cp^*_2V][B(C_6F_5)_4]$ (1c′). Fluorobenzene (1.5 mL) was added to a mixture of 55.0 mg (0.16 mmol) of Cp^*_2VMe and 125.7 mg (0.16 mmol) of $[PhNMe_2H][B(C_6F_5)_4]$. The resulting solution was layered with cyclohexane (3 mL), which afforded 140.2 mg (0.14 mmol, 89%) of red crystals after slow diffusion of the two solvents, removal of the supernatant, and washing with pentane (2 × 1 mL). Anal. Calcd for $C_{44}H_{30}BF_{20}V$: C, 52.83; H, 3.02. Found: C, 52.14; H, 3.04.[37]

$[Cp^*_2Sc(THF)_2][BPh_4]$ (5a). THF (1 mL) was added to a mixture of Cp^*_2ScMe (61.3 mg, 0.19 mmol) and $[PhNMe_2H][BPh_4]$ (76.1 mg, 0.17 mmol). Pentane (3 mL) was carefully layered on top of the resulting yellow reaction mixture, affording 85.2 mg (0.11 mmol, 65%) of yellow crystals of $[Cp^*_2Sc(THF)_2][BPh_4]$ after slow mixing of the two solvents by diffusion. ^1H NMR (THF-d_8, 200 MHz, room temperature): δ 7.29 (m, 8H, BPh_4), 6.87 (t, 7.3 Hz, 8H, BPh_4), 6.72 (t, 7.3 Hz, 4H, BPh_4), 3.58 (t, 6.1 Hz, THF), 1.93 (s, 30H, Cp*), 1.77 (t, 6.1 Hz, THF). Anal. Calcd for $C_{52}H_{66}BO_2Sc$: C, 80.28; H, 8.55; Sc, 5.66. Found: C, 79.98; H, 8.61; Sc, 5.70.

$[Cp^*_2Ti(THF)][BPh_4]$ (5b). THF (2 mL) was added to a mixture of 52.4 mg (0.16 mmol) of Cp^*_2TiMe and 68.4 mg (0.15 mmol) of $[PhNMe_2H][BPh_4]$. When no further gas evolution was observed (after 15 min), cyclohexane (3 mL) was layered carefully on top of the green reaction mixture. Diffusion of the two layers resulted in the deposition of $[Cp^*_2Ti(THF)][BPh_4]$. THF was obtained as green crystals. The product was isolated (57.3 mg, 0.07 mmol, 47%) by decanting the supernatant and drying at reduced pressure. ^1H NMR (THF-d_8, 200 MHz, room temperature): δ 11.70 (br, $\Delta\nu_{1/2} = 402$ Hz, Cp*), 7.6−6.6 (BPh_4). Anal. Calcd for $C_{52}H_{66}BO_2Ti$: C, 79.89; H, 8.51; Ti, 6.13. Found: C, 79.94; H, 8.43; Ti, 6.33.

$[Cp^*_2V(THF)][BPh_4]$ (5c). THF (1 mL) was added to a mixture of 58.2 mg (0.17 mmol) of Cp^*_2VMe and 70.2 mg (0.16 mmol) of $[PhNMe_2H][BPh_4]$. The resulting green solution was carefully layered with 3 mL of cyclohexane, affording 94.4 mg (83%) of green crystals of $[Cp^*_2V(THF)][BPh_4]$.^1H NMR (THF-d_8, 200 MHz, room temperature): δ 7.7−6.5 (*Ph*B). Anal. Calcd for $C_{48}H_{58}BOV$: C, 80.89; H, 8.20; V, 7.15. Found: C, 80.76; H, 8.26; V, 7.10.

Computational Studies. Calculations were performed using the Turbomole program,[38a,b] coupled to a PQS Baker optimizer.[39] Geometries were fully optimized at the bp86[40]/RIDFT[41] level using the Turbomole SV(P) basis set[38c,d] on all atoms. The energies are relative to the base-free metallocene cations and do not include zero-point energies or thermal corrections, and the anions have been omitted.

Acknowledgment. This investigation was supported by The Netherlands Foundation for the Chemical Sciences (CW) with financial aid from The Netherlands Organization for Scientific Research (NWO).

Supporting Information Available: Full experimental procedures and characterization data for all new compounds; complete ref 38a; computational details (extended geometric and energy data and representations of HOMO/SOMO and spin density); and X-ray crystallographic data (details of the refinements and CIF). This material is available free of charge via the Internet at http://pubs.acs.org.

JA054544I

(38) (a) Ahlrichs, R. et al. *Turbomole*, version 5; Theoretical Chemistry Group, University of Karlsruhe, January 2002. (b) Treutler, O.; Ahlrichs, R. *J. Chem. Phys.* **1995**, *102*, 346. (c) Turbomole basis set library. *Turbomole*, version 5; see 38a. (d) Schäfer, A.; Horn, H.; Ahlrichs, R. *J. Chem. Phys.* **1992**, *97*, 2571.
(39) (a) *PQS*, version 2.4; Parallel Quantum Solutions: Fayetteville, AR, 2001; the Baker optimizer is available separately from PQS upon request. (b) Baker, J. *J. Comput. Chem.* **1986**, *7*, 385.
(40) (a) Becke, A. D. *Phys. Rev. A* **1988**, *38*, 3089. (b) Perdew, J. P. *Phys. Rev. B* **1986**, *33*, 8822.
(41) Eichkorn, K.; Weigend, F.; Treutler, O.; Ahlrichs, R. *Theor. Chem. Acc.* **1997**, *97*, 119.